

1 **Neighbourhood species richness and drought-tolerance traits modulate tree**
2 **growth and $\delta^{13}\text{C}$ responses to drought**

3 *Florian Schnabel^{1,2*}, Kathryn E. Barry^{1,2,3}, Susanne Eckhardt², Joannès Guillemot^{4,5,6}, Heike*
4 *Geilmann⁷, Anja Kahl², Heiko Moossen⁷, Jürgen Bauhus⁸, Christian Wirth^{1,2,7}*

5

6 ¹German Centre for Integrative Biodiversity Research (iDiv) Halle-Jena-Leipzig, Leipzig,
7 Germany

8 ²Systematic Botany and Functional Biodiversity, University of Leipzig, Leipzig, Germany

9 ³Ecology and Biodiversity, Institute of Environmental Biology, Department of Biology, Utrecht
10 University, Utrecht, Netherlands

11 ⁴CIRAD, UMR Eco&Sols, Piracicaba, SP, Brazil

12 ⁵Eco&Sols, Univ Montpellier, CIRAD, INRAE, Institut Agro, IRD, Montpellier, France

13 ⁶Department of Forest Sciences, ESALQ, University of São Paulo, Piracicaba, São Paulo,
14 Brazil

15 ⁷Max Planck Institute for Biogeochemistry, Jena, Germany

16 ⁸Chair of Silviculture, Faculty of Environment and Natural Resources, University of Freiburg,
17 Freiburg, Germany

18 *Corresponding author: Florian Schnabel, Systematic Botany and Functional Biodiversity
19 University of Leipzig, Johannisalle 21, 04103 Leipzig, Germany, florian.schnabel@idiv.de

20

21 **Keywords:** biodiversity-ecosystem functioning, climate change, functional traits, plant–plant
22 interactions, tree rings, carbon isotopes, mixed-species forest, global change ecology

23

24

25 **Abstract**

26 **1.** Mixed-species forests are promoted as a forest management strategy for climate change
27 mitigation and adaptation because they are more productive and can be more resistant and
28 resilient than monospecific forests under drought stress. However, the trait-based mechanisms
29 driving these properties remain elusive, making it difficult to predict which functional identities
30 of species best improve tree growth and decrease tree physiological water stress under drought.

31 **2.** We investigated tree growth and physiological stress responses (i.e. increase in wood carbon
32 isotopic ratio; $\delta^{13}\text{C}$) to changes in climate-induced water availability (wet-to-dry years) along
33 gradients in neighbourhood tree species richness and drought-tolerance traits. Using tree cores
34 from a large-scale biodiversity experiment, we tested the overarching hypothesis that
35 neighbourhood species richness increases growth and decreases $\delta^{13}\text{C}$. We further hypothesized
36 that the abiotic (i.e. climatic conditions) and the biotic context modulate these biodiversity-
37 ecosystem functioning relationships. We characterized the biotic context using drought-
38 tolerance traits of focal trees and their neighbours. These traits are related to cavitation
39 resistance vs. resource acquisition and stomatal control.

40 **3.** We found that tree growth increased with neighbourhood species richness. However, we did
41 not observe a universal relief of water stress in species-rich neighbourhoods, nor an increase in
42 the strength of the relationship between richness and growth and between richness and $\delta^{13}\text{C}$
43 from wet-to-dry years. Instead, these relationships depended on both the traits of the focal trees
44 and their neighbours. At either end of each drought-tolerance gradient, species responded in
45 opposing directions during drought and non-drought years.

46 **4. Synthesis.** We report that the biotic context can determine the strength and nature of
47 biodiversity-ecosystem functioning relationships in experimental tree communities. We derive
48 two key conclusions: (1) drought-tolerance traits of focal trees and their neighbours can explain
49 divergent tree responses to drought and diversity, and (2) contrasting, trait-driven responses of
50 tree species to wet vs dry climatic conditions can promote forest community stability. Mixing

51 tree species with a range of drought-tolerance traits may therefore increase forest productivity
52 and stability.

53

54 **Introduction**

55 Forests are experiencing widespread mortality events due to climate extremes such as droughts
56 across all biomes (Hammond et al., 2022; Hartmann et al., 2022). Droughts are predicted to
57 increase in frequency and intensity with climate change (IPCC, 2014), threatening many
58 ecosystem services that forests provide, including their capacity to mitigate climate change
59 through carbon sequestration and storage (Anderegg et al., 2020). Large-scale forest restoration
60 initiatives such as the Bonn Challenge, which aims to restore 350 Mha of forests by 2030 to
61 mitigate climate change (Brancalion et al., 2019), need to optimize productivity and thus carbon
62 storage while at the same time increasing these restored forests' stability against climate
63 extremes. One key management strategy suggested to achieve this desired synergy between
64 productivity and stability is to establish and maintain tree species mixtures instead of
65 monocultures (Messier et al., 2021; Schnabel et al., 2019).

66

67 There is now accumulating evidence that species-rich forests provide higher levels and higher
68 stability of various ecosystem functions than species-poor or monospecific forests (del Río et
69 al., 2022; Messier et al., 2021; Schnabel et al., 2021; van der Plas, 2019). These positive species
70 richness effects, for instance on tree growth, may be more pronounced under stress (Bertness
71 & Callaway, 1994; Forrester & Bauhus, 2016) and have been shown to increase in dry
72 compared to wet years (Fichtner et al., 2020; Schnabel et al., 2019). However, studies on net
73 tree mixture responses to drought have produced divergent results, including positive, neutral
74 and negative diversity effects under drought (reviewed by Grossiord (2020)) and we thus do
75 not yet know when diversity is beneficial for forest functioning under drought.

76

77 Understanding the mechanisms driving this variation in biodiversity-ecosystem functioning
78 (BEF) relationships may be best achieved through examining tree responses to drought and how
79 they are modulated by tree species richness at the relevant scale at which tree-tree interactions
80 take place, the local neighbourhood (Trogisch et al., 2021). This is because neighbourhood
81 analyses allow studying diversity effects in concert with other factors such as tree size and
82 competition, which may also influence growth, and to (partly) disentangle their respective
83 contributions to growth (Forrester & Pretzsch, 2015; Stoll & Newbery, 2005). For instance,
84 neighbourhood analyses showed that mean tree growth across species increases with tree
85 neighbourhood species richness (hereafter called ‘NSR’) despite positive and negative NSR
86 effects on the growth of individual species (Fichtner et al., 2018; Schnabel et al., 2019).

87

88 The recent history of these neighbourhood interactions can be analysed in the tree ring record
89 of a focal tree, which captures its response to neighbours and climatic variation (Schweingruber,
90 1996; Vitali, Forrester, & Bauhus, 2018). The width of annual growth rings is an indicator of a
91 tree’s reaction to climate, with reduced growth in dry compared to wet years indicating
92 increased drought stress (Schwarz et al., 2020). In addition to growth, the isotopic ratio of
93 $^{13}\text{C}/^{12}\text{C}$ in wood (hereafter ‘ $\delta^{13}\text{C}$ ’) is a principal indicator of a tree’s physiological reaction to
94 water limitation and drought stress (Grossiord et al., 2014; Jucker et al., 2017). An increase in
95 $\delta^{13}\text{C}$ indicates drought stress, as trees increasingly use the heavier ^{13}C when stomata close to
96 avoid water loss from transpiration (Farquhar, Ehleringer, & Hubick, 1989; Grossiord et al.,
97 2014). We expect that the mixed results on tree species richness effects on growth and $\delta^{13}\text{C}$
98 under drought reported in former studies (see above; Grossiord (2020)) may be explained by
99 species-specific water-use strategies. We expect this because water-use strategies, which can
100 be studied using functional traits, impact how species respond to their surrounding abiotic (i.e.
101 climatic conditions) and biotic environment (i.e. their tree neighbours) (Forrester, 2017).

102

103 Among other relevant traits, two key traits proposed to influence tree responses to drought are
104 cavitation resistance and the stringency of stomatal control (McDowell et al., 2008), which we
105 collectively refer to as ‘drought-tolerance traits’ (Schnabel et al., 2021). Xylem resistance to
106 cavitation reduces embolism risk in vessels, which impair water transport and, at advanced
107 stages, induce desiccation and, ultimately, tree death (Choat et al., 2012). Cavitation resistance
108 is often quantified as the water potential where 50% of conductivity is lost due to cavitation
109 (Ψ_{50} ; Choat et al., 2012). Moreover, cavitation resistance has been shown to be associated with
110 classic traits of the leaf economics spectrum in tropical tree species (Guillemot et al., 2022) and
111 thus with resource use strategies. Accordingly, cavitation-sensitive species have traits
112 indicative of acquisitive resource use (Fichtner et al., 2020; Schnabel et al., 2021). In addition
113 to cavitation resistance, stomatal control differs among species (see McDowell et al., 2008):
114 some species close their stomata early during water shortages to avoid transpirational water
115 loss, whereas others keep their stomata open despite increasingly negative water potentials and
116 increasing cavitation risks. In line with current perspectives (Martínez-Vilalta & Garcia-Forner,
117 2017), we use physiological traits such as stomatal conductance and its control under increasing
118 vapour pressure deficits (VPD) to quantify stomatal control as a gradient from water savers,
119 which close their stomata early as water stress develops, to water spenders, which keep their
120 stomata open despite increasing VPD (Kröber & Bruelheide, 2014; Kröber, Zhang, Ehmig, &
121 Bruelheide, 2014). Diversity in these traits, hereafter referred to as ‘resistance-acquisition’ and
122 ‘stomatal control’ traits, has been recently shown to be positively related to the stability of forest
123 community productivity under highly variable climatic conditions (Schnabel et al., 2021).
124 However, these traits have not been used in a comprehensive framework to characterize the
125 functional identity of focal trees (i.e. their traits) and their neighbours (i.e. the neighbourhood
126 mean values of traits) to understand how these functional identities influence growth and wood

127 $\delta^{13}\text{C}$ responses to the interactive effects of NSR and contrasting climatic conditions (such as
128 particularly dry and wet years).

129

130 A focal trees' functional (trait) identity, hereafter 'focal tree traits', may be crucial to understand
131 responses of tree growth and $\delta^{13}\text{C}$ to the interactive effects of drought and NSR. Consistent
132 with this expectation, Fichtner et al. (2020) showed that positive NSR effects on aboveground
133 wood production were strongest for cavitation-sensitive species during drought. Moreover,
134 another study, even though conducted in a wet year, found that increasing acquisitiveness and
135 NSR caused decreased $\delta^{13}\text{C}$ values in tree twig tissues, indicating enhanced water availability
136 in diverse neighbourhoods (Jansen, Oheimb, Bruelheide, Härdtle, & Fichtner, 2021). We expect
137 growth to be more strongly related to resistance-acquisition traits and thus the leaf economics
138 spectrum (Reich, 2014). Alternatively, we expect wood $\delta^{13}\text{C}$ to be primarily controlled by
139 stomata aperture (Farquhar et al., 1989) and thereby stomatal control traits.

140

141 The trait identity of a focal trees' neighbours, hereafter 'neighbour traits', may also influence
142 the growth and $\delta^{13}\text{C}$ of focal trees through interactions (Fortunel, Valencia, Wright, Garwood,
143 & Kraft, 2016; Trogisch et al., 2021). In this view, neighbour traits may alter water use and
144 with this local water availability. For example, during drought, growth reductions in water
145 spenders may be lower and $\delta^{13}\text{C}$ increases smaller when growing with more water-saving
146 neighbours because the reduced stomatal conductance of the latter may decrease overall water
147 consumption and thus drought stress in focal trees (Forrester, 2017). Conversely, being
148 surrounded by water spending neighbours during drought may amplify focal tree growth
149 reductions and $\delta^{13}\text{C}$ increases. In summary, we expect that the abiotic context (i.e. climatic
150 conditions) and the biotic context jointly modulate growth and $\delta^{13}\text{C}$ responses to NSR. We
151 characterized this biotic context, which has received little attention compared to the many
152 studies that examined the abiotic context dependency of BEF relationships (e.g. Forrester

153 & Bauhus, 2016; Grossiord, 2020; Jucker et al., 2016; Paquette & Messier, 2011), as traits of
154 focal trees and as traits of their neighbours.

155

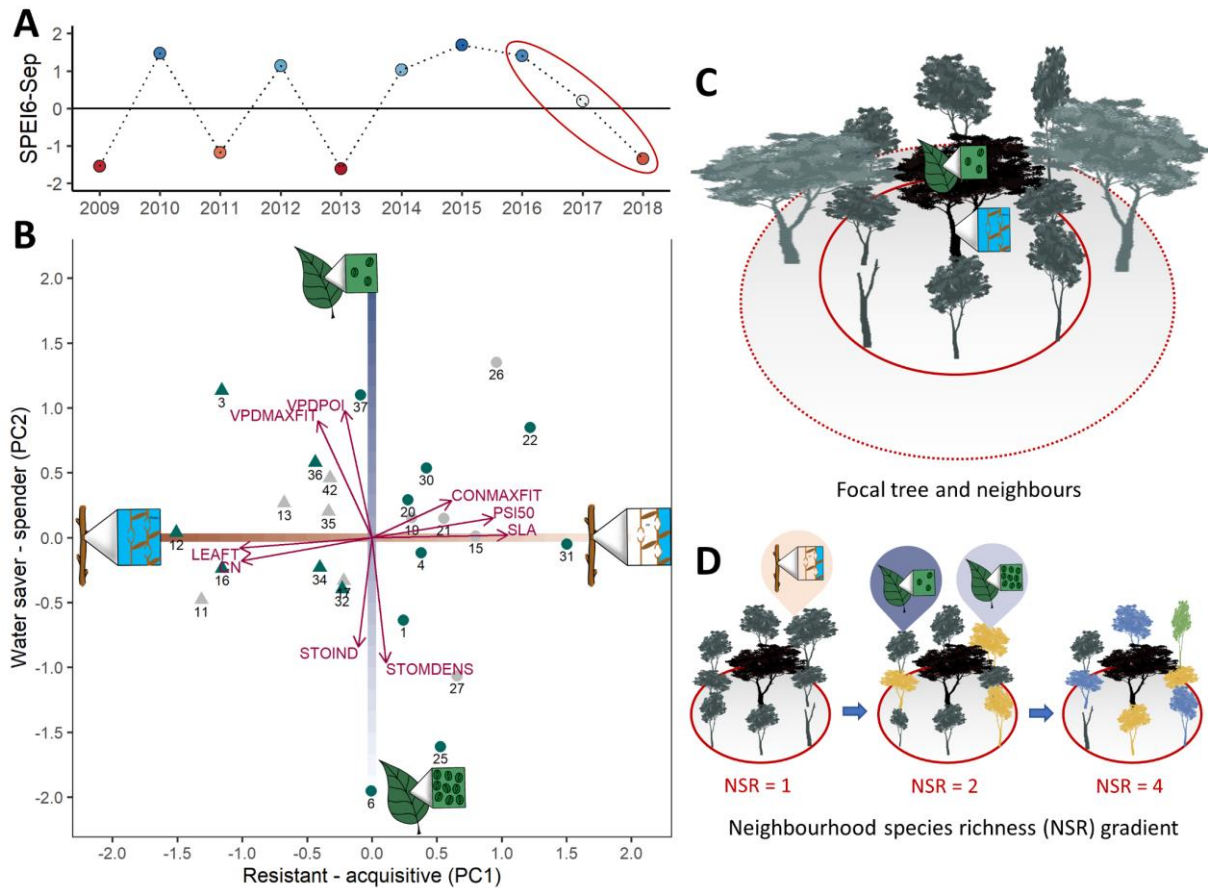
156 Here, we aim to understand how drought-tolerance traits influence the relationship between
157 NSR and growth, and NSR and $\delta^{13}\text{C}$ under variable climatic conditions. We use trait-based
158 neighbourhood models that account for NSR as well as focal tree and neighbour traits and
159 examine how they jointly influence focal tree growth and $\delta^{13}\text{C}$ in a climatically dry, normal and
160 wet year (Fig. 1) in a large-scale sub-tropical tree biodiversity-ecosystem functioning
161 experiment (BEF-China experiment; Bruelheide et al., 2014; Huang et al., 2018). Specifically,
162 we tested the following hypothesis:

163 **H1:** NSR increases growth and decreases $\delta^{13}\text{C}$ of focal trees, and the strength of this diversity
164 effect increases from wet to dry years.

165 **H2:** Drought-tolerance traits of focal trees determine the relationship between NSR and growth,
166 and NSR and $\delta^{13}\text{C}$ under variable climatic conditions. Specifically, during drought, NSR
167 increases growth and decreases $\delta^{13}\text{C}$ for acquisitive and water-spending species, while the
168 reverse pattern is found for cavitation-resistant and water-saving species.

169 **H3:** Drought-tolerance traits of neighbours influence the effect of climate on focal tree growth.
170 Specifically, during drought, acquisitive and water-spending neighbours amplify drought stress.

171



172

173 Fig. 1 Study design. (A) Climatic characterisation of the study years 2016 (wet), 2017 (intermediate)

174 and 2018 (dry) based on the Standardised Precipitation-Evapotranspiration Index (SPEI) for the

175 principal vegetation period (April-September) since the establishment of the BEF-China experiment

176 (2009). The wet-to-dry study years under investigation are highlighted with a red oval. Blue points

177 indicate wetter and red points drier conditions compared to the long-term mean (1901-2019); values

178 below -1 and above 1 can be considered exceptional. (B) Species selection via their drought-tolerance

179 traits based on principal component analysis (PCA) adapted from Schnabel et al. (2021). PC1 reflects a

180 resistance-acquisition gradient running from cavitation-resistant (low Ψ_{50} , tough leaves (LEAFT), high

181 C/N ratio) to acquisitive species (high Ψ_{50} , high specific leaf area (SLA), high maximum stomatal

182 conductance (CONMAXFIT)). PC2 reflects a stomatal control gradient running from water spenders

183 with late stomata closure under decreasing vapour pressure deficits (VPDs) (high VPD at the point of

184 inflection of modelled stomatal conductance (VPDPOI), high VPD at CONMAXFIT (VPDMAXFIT))

185 to water savers with fast stomata closure (high stomatal density (STODENS), high stomatal index

186 (STOIND)). The sketches illustrate the trait gradients: (PC1) high vs low cavitation resistance, (PC2)

187 water-spending *vs* water-saving stomatal control (few versus abundant stomata). We selected 15 species
188 to cover the trait space (highlighted in green). See Table S1 for a list of tree species represented here by
189 codes and Table S2 for details on the traits. (C) Tree neighbourhood design. We extracted increment
190 cores from focal trees (black tree) of the 15 species and inventoried their 1st and 2nd order neighbours
191 (grey trees). (D) Neighbourhood species richness (NSR) gradient. We sampled focal trees and their
192 neighbours to create a realised NSR gradient of 1-, 2- and 4-neighbour species. The sketches in C and
193 D illustrate that we examined the influence of focal tree and neighbour traits on the relationships between
194 NSR, climate and growth as well as $\delta^{13}\text{C}$ for both trait gradients (resistance-acquisition and stomatal
195 control). For additional details on the study design, see methods.

196

197 **Materials and Methods**

198 **Study site and experimental design**

199 We sampled trees in a large-scale tree biodiversity-ecosystem functioning experiment located
200 in Xingangshan, Dexing, Jiangxi province, China (29°08'N to 29°11'N, 117°90'E to 117°93'E),
201 the BEF-China experiment (Bruehlheide et al., 2014; Huang et al., 2018). The experiment has
202 two sites: A and B, each approximately 20 ha in size. The sites are characterised by a
203 subtropical, monsoon climate with a mean annual temperature of 16.7 °C and a yearly
204 precipitation sum of 1821 mm (Yang et al., 2013), with distinct differences between seasons.
205 Summers are humid, with most annual precipitation falling from April to July, while winters
206 are drier and cold (Gheyret et al., 2021). Deciduous and evergreen broadleaved tree species
207 dominate the hyperdiverse native forests of the study region, sometimes interspersed with
208 conifers (Bruehlheide et al., 2014). The high diversity can be attributed, at least partially, to the
209 location of the region in the transition zone of tropical and temperate climates with their
210 respective flora (Shi, Michalski, Welk, Chen, & Durka, 2014; Wang, Kent, & Fang, 2007). This
211 resulted also in a high diversity of water-use strategies among tree species, which makes these
212 forests ideal for studying species response strategies to variable climatic conditions (Kröber et

213 al., 2014; Kröber & Bruelheide, 2014; Schnabel et al., 2021). Based on a pool of 40 native
214 evergreen and deciduous broadleaf tree species, experimental tree species richness gradients
215 were created with 1, 2, 4, 8, 16 and 24 tree-species mixtures. Species were assigned to different
216 extinction scenarios following a broken-stick design, ensuring that all species were represented
217 at each species richness level (Bruelheide et al., 2014; Huang et al., 2018). In 2009 (site A) and
218 2010 (site B), overall, 226,400 individual trees were planted at a distance of 1.29 meters (Fig.
219 1) on plots with a size of $25.8 \times 25.8 \text{ m}^2$, with 400 trees being planted per plot. Species
220 compositions and tree positions within plots were randomly assigned to each plot.

221

222 **Climate-based selection of study years**

223 We selected three study years with contrasting climatic conditions, a comparably wet (2016),
224 an intermediate (2017) and a particularly dry year (2018). We selected consecutive years to
225 minimise other factors than climate that may influence growth and $\delta^{13}\text{C}$, such as changes in
226 stand structure. We used the standardised precipitation evapotranspiration index (SPEI)
227 (Vicente-Serrano, Beguería, & López-Moreno, 2010) calculated from a high-resolution time-
228 series of interpolated climate station data (CRU TS v4.04; Harris, Osborn, Jones, & Lister,
229 2020) to characterise climatic conditions. The SPEI represents a standardised climatic water
230 balance of precipitation minus potential evapotranspiration (PET). We selected study years
231 based on climatic conditions alone without taking tree growth reductions into account (see
232 suggestions by Schwarz et al. (2020)) by comparing the SPEI series calculated for the three
233 months of the peak vegetation period (SPEI3, April-July) for the six months of the entire
234 vegetation period (SPEI6, April-September) and the twelve months of a whole year since the
235 end of the vegetation period of the preceding year (SPEI12, October-September), with a climate
236 reference period from 1901-2019 (Fig. 1A, Fig. S1). The subtropical vegetation period ranges
237 from April-September with peak growth at the end of April (Gheyret et al., 2021), which
238 corresponds well with the selected lengths of periods for which SPEI was calculated. All

239 periods (SPEI3, SPEI6, SPEI12) showed the same pattern of decreasing SPEI values from
240 2016-2017-2018 (Fig. S1), with drought severity in the dry year being comparable to drought
241 conditions in the last 40 years (Fig. S2). In addition, we also examined intra-annual and non-
242 standardized climatic water balances (Fig. S3).

243

244 **Species selection via drought-tolerance traits**

245 We used this experimental set-up to select tree species along two principal trait gradients related
246 to resistance-acquisition and stomatal control traits (Fig. 1B) which allowed us to study their
247 relative contributions to tree growth and $\delta^{13}\text{C}$. For this purpose, we relied on species-specific
248 trait data related to cavitation resistance, resource acquisitiveness and stomatal control
249 measured in the experiment (Table S2; Kröber et al., 2014; Kröber & Bruelheide, 2014). Trait
250 data were analysed with principal component analysis (PCA), which partitioned the variation
251 in drought-tolerance traits into two orthogonal trait gradients, a resistance-acquisition (PC1)
252 and stomatal control (PC2) trait gradient (see Schnabel et al. (2021) for details). In brief, we
253 quantified cavitation resistance as the water potential (Ψ_{50}) at which 50% of xylem conductivity
254 is lost due to cavitation, which is a key physiological trait to characterise a species drought
255 tolerance (Choat et al., 2012). In our study system, Ψ_{50} is related to classic traits of the leaf
256 economics spectrum (Reich, 2014) in that cavitation-resistant species (low Ψ_{50} values) are also
257 characterised by traits indicative of conservative resource use (tough leaves and high C/N ratio),
258 while cavitation-sensitive species (less negative Ψ_{50} values) have traits indicative of acquisitive
259 resource use such as high specific leaf area (SLA) and high maximum stomatal conductance
260 (g_{smax}) (Fig. 1B). Including this gradient provided a balanced selection of deciduous and
261 evergreen species. Second, we quantified stomatal control using modelled curves of stomatal
262 conductance (g_{s}) under increasing vapour pressure deficits (VPD) and morphological traits
263 (stomatal density and stomatal index, the product of stomatal density and size) (Fig. 1B). Water
264 savers are characterised by a high stomatal density, high stomatal index values, and a fast down-

265 regulation of their conductance under increasing VPD. In contrast, water spenders down-
266 regulate their stomatal conductance only at high VPD (high VPD_{MAXFIT} and VPD_{POI}).

267

268 In 2019, we selected 15 tree species to cover the trait space as well as possible by choosing
269 species at the extremes of both gradients (2 species at each end) and at intermediate values of
270 trait expression (Fig. 1B). We used the species PCA scores on the resistance-acquisition and
271 stomatal control trait gradient as focal tree traits, hereafter referred to as ‘focal tree resistance-
272 acquisition traits’ and ‘focal tree stomatal control traits’. We restricted this selection to 25 tree
273 species (of 40 in total), which featured mid- to fast growth rates in our experiment (Li, Kröber,
274 Bruelheide, Härdtle, & Oheimb, 2017), showed distinct radial growth rings (Böhnke, Kreißig,
275 Kröber, Fang, & Bruelheide, 2012), and had comparably good survival rates to ensure sufficient
276 tree and sample size for coring. As species pools in the BEF-China experiment overlap only
277 partly between sites A and B (Bruelheide et al., 2014), we sampled seven species at site A,
278 seven at site B and one species (*Schima superba*) at both sites to test for potential differences
279 between sites (i.e. eight total species at each site).

280

281 **Focal trees and their neighbourhood**

282 We used focal trees and their neighbours to create a realised neighbourhood species richness
283 (NSR) gradient of 1-, 2- and 4-neighbour species (Fig. 1C,D). In the field, we randomly selected
284 10 focal trees (7 trees for final analysis and 3 trees as backup) per species (N=15) and NSR
285 level (N=3), which resulted in 485 trees in total (one species was sampled at both sites). Focal
286 trees were selected outside the plot’s inventoried core area to avoid interference with other
287 projects and not near plot borders unless the adjacent plot contained species for which complete
288 trait information existed. We defined NSR as the realised neighbourhood species richness at
289 sampling (2019). In a few cases (*Idesia polycarpa*, *Triadica cochinchinensis*), we used the
290 original plot-level richness at the time of planting due to the high mortality of focal and

291 neighbour species. For NSR=1 and NSR=2, we selected trees only from plots with the
292 respective plot-level design richness (monocultures and 2-species mixtures). The random
293 planting design of BEF-China substantially reduced the likelihood of finding high-diversity
294 neighbourhoods. At NSR=4, we thus also selected plots with a higher plot-level design richness,
295 i.e. 8- and 16-species mixtures in this order of preference. Sampling neighbourhoods with four
296 species only in 4-species mixtures was impossible due to the high mortality of neighbour
297 species. We sampled focal trees in as many different plots and species compositions as possible
298 to increase the generality of our results (N=122 plots) and avoided overlapping neighbourhoods
299 to minimise spatial-autocorrelation. We used a focal tree threshold diameter at breast height
300 (dbh, at 1.3m) of > 8cm (in a few cases ~6cm) to avoid damaging the trees when extracting
301 cores for analysis (see below). For each focal tree, we recorded its position, species' identity
302 and dbh. When trees had multiple stems, the stem diameters of the two largest stems were
303 recorded to calculate the sum of the basal areas of both stems.

304

305 We defined a focal tree's neighbourhood as all alive direct neighbours (occupying the
306 immediately adjacent original planting space; maximum eight trees) and second-order
307 neighbours (occupying the original planting spaces one further out from the direct neighbours)
308 if their crown and the focal tree's crown interacted (Fig. 1C). For each neighbour, we recorded
309 its position, species' identity, and dbh and visually estimated the height difference of
310 neighbours compared to focal trees as a measure of shading by neighbours. We used these data
311 to characterise the competitive environment of focal trees using eight different diameter-,
312 height-, and distance-based neighbourhood competition indices frequently used in other studies
313 (Table S3). Tree basal area (cm^2 , based on dbh), and in the case of multi-stemmed trees, the
314 sum of basal areas of individual stems was used in these analyses. We calculated neighbour
315 traits, i.e. the functional identity of a focal trees' neighbourhood, as the neighbourhood-
316 weighted mean (NWM) trait value of each neighbourhood for both gradients, hereafter called

317 ‘NWM of resistance-acquisition’ and ‘NWM of stomatal control’, similarly to the calculation
318 of community-weighted mean traits often used in BEF studies (see, e.g. Craven et al., 2018) as:
319

$$320 \quad NWM = \sum_{i=1}^n a_{ba\ i} t_i \quad (1)$$

321
322 Where a_{ba} is the abundance of species i measured as its basal area relative to the basal area of
323 the other neighbour species and t_i is the score of species i on the respective trait gradient (PCA
324 axes reflecting resistance-acquisition or stomatal control; Fig. 1).

325

326 **Tree growth and stable carbon isotopes**

327 We used tree growth and carbon isotopic ratios as indicators of focal tree responses to the
328 interactive effects of climate, NSR and drought-tolerance traits. We extracted one increment
329 core at dbh from each focal tree perpendicular to the slope (avoiding tension wood) using a 3-
330 threaded Haglöf increment borer with 3.5 mm core diameter. We extracted cores from the
331 largest stem and recorded tree diameter at the coring position if coring at dbh was not possible.
332 Cores were tightly wrapped in paper to avoid bending and dried for 72 hours at 70 °C. Core
333 surfaces were prepared with a core-microtome (Gärtner & Nievergelt, 2010) to visualise tree-
334 ring boundaries. Annual tree-ring width (mm) was measured using a LINTAB™ 6 system and
335 the TSAPWin Professional 4.64 program © 2002–2009 Frank Rinn / RINNTECH with a
336 measurement accuracy of 1/1000 mm. We measured each core twice and cross-compared series
337 within species to ensure the correct dating of rings. No master chronology per species could be
338 constructed owing to the short length of individual series (mostly 5-7 years). Tree-ring series
339 of 474 trees from 15 species could be dated (see Fig. S4 for an overview of wood anatomy).
340 Basal area increment (cm²) is less influenced by biological age trends than tree-ring width (see
341 Fig. S5 for a comparison). It is thus a more reliable indicator of temporal trends in tree growth,
342 particularly in young, open-grown trees like the ones examined here (Biondi & Qeadan, 2008).

343 Therefore, in the following, we present and discuss results based on basal area increment (also
344 referred to as growth). We present results for tree-ring width, which yielded similar results, in
345 the appendix. Basal area increment was calculated using tree-ring width, bark thickness and the
346 tree diameter at coring-position with the `bai.out()` function in the `dplR` package in R (Bunn et
347 al., 2020).

348

349 The carbon isotopic ratio in the wood of focal trees ($\delta^{13}\text{C}$) was quantified for the years 2016-
350 2018 on the same cores. The rings of the years were separated, their wood homogenised and
351 0.8 mg woody material was weighed and placed in tin capsules. We determined $\delta^{13}\text{C}$ in bulk
352 wood rather than extracted cellulose fraction, because both materials produce highly correlated
353 signals (Loader, Robertson, & McCarroll, 2003; Schulze et al., 2004). Carbon isotope analyses
354 were conducted on an elemental analyser (NA1110, CE Instruments, Milan, Italy) coupled to a
355 Delta+XL isotope ratio mass spectrometer (Thermo Finnigan, Bremen, Germany) via a
356 ConFlow III at the stable isotope laboratory (BGC-IsoLab) of the Max Planck Institute for
357 Biogeochemistry in Jena, Germany. We present carbon isotope ratio results as $\delta^{13}\text{C}$ values on
358 the VPDB-LSVEC scale (Coplen et al., 2006). The $\delta^{13}\text{C}$ values are reported in per mil (‰) by
359 multiplying the delta value by the factor 1000 (Coplen, 2011).

360

$$361 \quad \delta^{13}\text{C} = \left(\frac{\delta^{13}\text{C}(\text{sample})}{\delta^{13}\text{C}(\text{standard})} - 1 \right) \quad (2)$$

362

363 Samples were scaled against the in-house standard (acetanilide) with a $\delta^{13}\text{C}$ value of $-30.06 \pm$
364 0.1 ‰. Caffeine (caf-j3; $\delta^{13}\text{C}$: -40.46 ± 0.1 ‰) was analysed several times in each sequence as
365 quality control. Linearity, blank and drift corrections were done for each sequence according to
366 Werner and Brand (2001). We randomly remeasured a subset of samples to estimate
367 measurement precision. The mean standard-deviation of samples from the same year and tree

368 lay with 0.05 ± 0.03 ‰ well in the range of the in-house standard precision. We used the mean
369 of these repeated measurements in the further analyses.

370

371 Wood $\delta^{13}\text{C}$ is influenced both by stomatal aperture and CO_2 assimilation (Farquhar et al., 1989;
372 Grams, Kozovits, Häberle, Matyssek, & Dawson, 2007), with the latter being largely influenced
373 by shading from neighbouring trees and the former by water availability. One common
374 approach to separate the effects of water availability from shading on $\delta^{13}\text{C}$ is to analyse isotopic
375 signals in tree rings from (co-)dominant trees who experience no or only slight shading from
376 neighbours (Grossiord et al., 2014; Jucker et al., 2017). In contrast to a former study which did
377 not control for tree size and canopy position during sampling and consequently found strong
378 shading effects on $\delta^{13}\text{C}$ (Jansen et al., 2021), we aimed at maximizing the climate-induced water
379 availability signal in $\delta^{13}\text{C}$. We did this in two ways. First, our selection of species with mid- to
380 fast growth rates and the use of a minimum dbh of 8 cm (see above) resulted in a sample of (co-
381)dominant individuals. Second, to further reduce shading effects on focal trees and to
382 simultaneously ensure the same sample size across species and NSR levels, we carried out an
383 *a priori* selection of those focal trees that experienced least shading by their neighbourhood.
384 For that purpose, those focal trees with the highest sum of relative heights of neighbours (height
385 of focal tree minus height of neighbour) (see above) to select 7 trees per species, NSR-level and
386 site for statistical analysis. We constrained this selection to keep a minimum of two trees per
387 plot. The final, completely balanced dataset per species, NSR-level and year comprised 336
388 trees from 114 plots with at least two trees per plot (see Fig. S6 for an overview of basal area
389 increment and $\delta^{13}\text{C}$ values per species and NSR-level).

390

391 **Statistical analysis**

392 We used linear mixed-effects models (LMMs) to model growth (basal area increment and tree-
393 ring width) and wood $\delta^{13}\text{C}$ responses to the interactive effects of climate, NSR and drought-

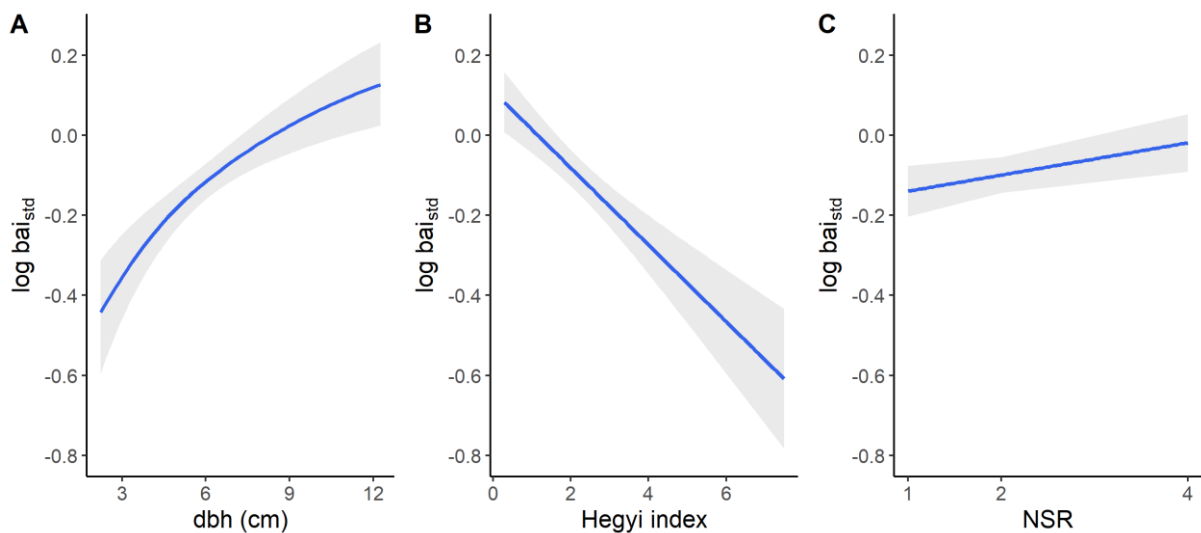
394 tolerance traits. Our modelling framework consisted of three main steps. First, we built trait-
395 independent neighbourhood models that accounted for the size of focal trees, its competition
396 with neighbours, climate and NSR, and the interaction between climate \times NSR as fixed effects.
397 We accounted for our experimental design through a nested random effect structure of focal
398 tree identity (to account for repeated measurements) nested within plot and site. We included
399 focal tree size as the log-transformed initial dbh (at the end of 2015) before our analysis period
400 (2016-2018), which we estimated using tree-ring width and the trees' dbh recorded in 2019.
401 We then tested eight neighbourhood competition indices (Table S3) and selected the best-
402 performing one via the Akaike Information Criterion (AIC). We accounted for differences in
403 average annual climatic conditions using year (2016-wet, 2017-intermediate and 2018-dry, Fig.
404 1A) as a fixed effect, coded as an integer variable as we expected linear trends. We also checked
405 for non-linear behaviour through alternative models with year as a categorical fixed effect. We
406 used years rather than SPEI-values as we only examined three years with a clear gradient in
407 climate-induced water availability. Reported relationships would be the same if using SPEI
408 values (checked via alternative LMMs with SPEI-values as a fixed effect). We selected the
409 most parsimonious random effect structure using the step function in lmerTest ($\alpha=0.2$, a
410 conservative choice), which retained tree identity and plot but not site as nested random effects
411 for models to explain growth and $\delta^{13}\text{C}$. We kept this random effect structure in all further
412 analyses. A separate analysis of *Schima superba*, the species sampled at both sites, confirmed
413 that growth and $\delta^{13}\text{C}$ responses did not differ between sites (supplementary analysis 1). Finally,
414 we selected the most parsimonious trait-independent neighbourhood model through backward
415 elimination of fixed effects ($\alpha=0.05$). In a second step, we examined how focal tree traits
416 modulate growth and $\delta^{13}\text{C}$ responses by including the 3-way interaction between NSR, climate
417 and either resistance-acquisition or stomatal control traits of focal trees and all potential 2-way
418 interactions as fixed effects in the trait-independent models of step 1. We selected the most
419 parsimonious focal tree trait model through backward elimination of fixed effects. Third, to

420 understand how neighbour traits modulate growth and $\delta^{13}\text{C}$, we included the 2-way interaction
421 of climate with either the resistance-acquisition or stomatal control traits of neighbours as fixed
422 effects in the trait-independent models (step 1) and again selected the most parsimonious model
423 structure via backward elimination of fixed effects. Hence, in contrast to former studies
424 (Fichtner et al., 2020; Jansen et al., 2021), we explicitly accounted for interactions between
425 focal trees and their neighbourhood on growth and $\delta^{13}\text{C}$ through modelling the effect of
426 neighbourhood species composition not as a random effect but as a fixed effect expressed
427 through the NWM of species' drought-tolerance traits. We used separate models for
428 understanding the effects of focal tree and neighbour traits (steps 2 and 3). The validity of this
429 choice was confirmed, as joint focal tree and neighbour trait models consistently dropped one
430 term (mostly neighbour traits), which was highly significant if examined alone. Across the
431 examined 15 species, we observed large species-specific differences in growth and particularly
432 in $\delta^{13}\text{C}$ (Fig. S6). As we were interested in relative species responses to the interactive effects
433 of NSR, climate and drought-tolerance traits and not in absolute species differences, we
434 standardised basal area increment and tree-ring width values by dividing each value by its
435 species' mean and $\delta^{13}\text{C}$ values by subtracting its species' mean in all analyses to reduce total
436 variance in the data, referred to as bai_{std} , trw_{std} and $\Delta\delta^{13}\text{C}$, respectively. Alternative models with
437 species identity as a random effect yielded similar results (results not shown). LMMs were fit
438 in R version 4.1.2 with the packages lme4 (Bates, Mächler, Bolker, & Walker, 2015) and
439 lmerTest (Kuznetsova, Brockhoff, & Christensen, 2017). Model assumptions (normality and
440 heteroscedasticity) were visually checked via quantile-quantile plots and through examining
441 model residuals. We used a log transformation for basal area increment and a square-root
442 transformation for tree-ring width to normalise residuals, centred and scaled all predictors (via
443 subtracting μ and dividing by σ) except year and NSR before analysis and used an α of 0.05 for
444 reporting significant effects.

446 Results

447 Using trait-independent models, we found that focal tree growth (expressed as basal area
448 increment) increased with the logarithm of tree size ($t = 5.01$, $P < 0.001$), decreased with
449 competition by neighbours ($t = -5.91$, $P < 0.001$), and increased with NSR by 11.4% from 1-
450 species to 4-species neighbourhoods ($t = 2.29$, $P = 0.024$) (Fig. 2, Table S4). The Hegyi index,
451 which accounts for neighbour distance and basal area relative to the focal tree, was the best-
452 performing competition index (Table S5). NSR effects on growth did not change with annual
453 climatic conditions, nor did we observe absolute differences in growth across years (2016-wet,
454 2017-intermediate, 2018-dry). The trait-independent models for $\delta^{13}\text{C}$ in the wood of focal trees
455 showed a linear decrease in $\delta^{13}\text{C}$ from the wet-to-dry year ($t = -9.06$, $P < 0.001$; Fig. S7, Table
456 S6). Neither tree size, competition, NSR, nor the interaction between NSR and year
457 significantly affected $\delta^{13}\text{C}$ (Tables S6,7).

458



459

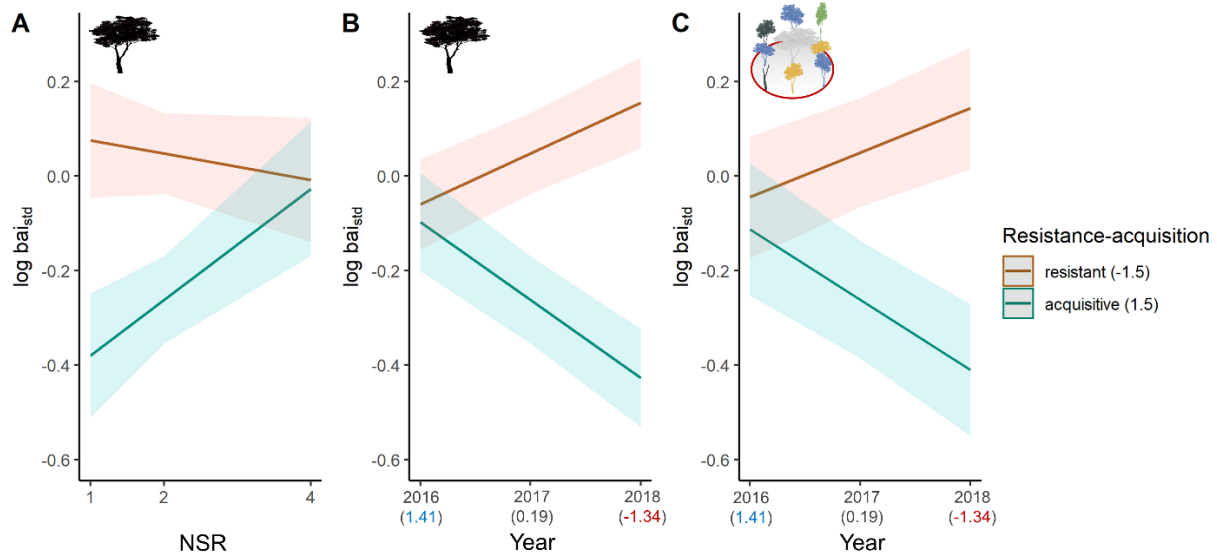
460 Fig. 2 Effects of tree size (dbh), neighbourhood competition (Hegyi index) and neighbour
461 hood species richness (NSR) on the logarithm of focal tree basal area increment (bai_{std}). The blue lines are mixed-
462 effects model fits and grey bands show a 95% confidence interval. See Table S4 for details on the fitted
463 model.

464

465 **The effect of drought-tolerance traits on tree growth**

466 Using trait-dependent models to explain focal tree growth, we found that the resistance-
467 acquisition traits of focal trees significantly modulated the relationship between NSR and
468 growth and between climate and growth (Fig. 3A,B, Table S8). With increasing NSR,
469 acquisitive, cavitation-sensitive species grew 29.7 % more in 4-species compared to 1-species
470 neighbourhoods, whereas growth of conservative, cavitation-resistant species decreased by
471 8.9% in 4-species compared to 1-species neighbourhoods (NSR \times focal tree resistance-
472 acquisition traits, $t = 2.45$, $P = 0.015$; Fig. 3A). Growth of resistant species increased from the
473 wet-to-dry year, while it declined in acquisitive species (year \times focal tree resistance-acquisition
474 traits, $t = -6.84$, $P < 0.001$; Fig. 3B). We also found that the resistance-acquisition traits of focal
475 trees tended to induce contrasting relationships between NSR, climate and growth. Still, this 3-
476 way interaction was only marginally significant (NSR \times year \times focal tree resistance-acquisition
477 traits, $t = -1.75$, $P = 0.080$; Fig. S8, Table S10): Effects of the resistance-acquisition traits of
478 focal trees were strongly contrasting (acquisitive species grew better and resistant species grew
479 less with increasing NSR) during the wet year, while effects in the dry year were weaker but
480 predominately positive (acquisitive species still grew more with increasing NSR, while NSR
481 did not affect the growth of resistant species). Notably, the resistance-acquisition traits of
482 neighbours significantly influenced growth responses; that is, focal trees in a neighbourhood
483 dominated by resistant species grew more from the wet-to-dry year, while focal trees in an
484 acquisitive neighbourhood grew less (year \times NWM of resistance-acquisition, $t = -4.17$, $P <$
485 0.001 ; Fig. 3C, Table S9).

486



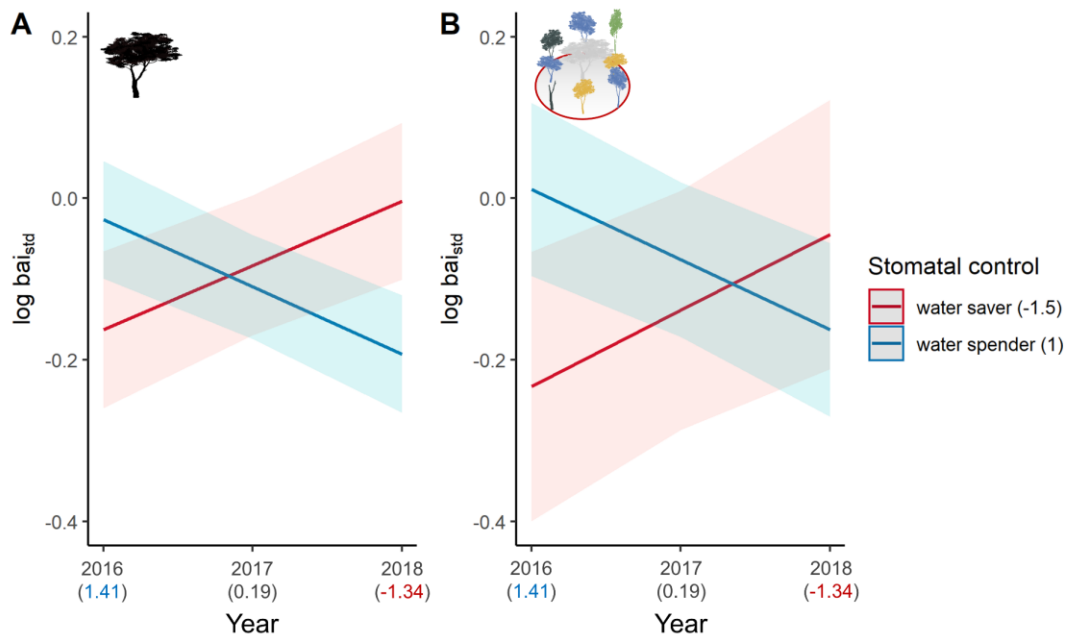
487

488 Fig. 3 Modulation of the relationship between neighbourhood species richness (NSR) and growth and
489 between climate and growth by resistance-acquisition traits. Lines represent linear mixed-effects model
490 fits and coloured bands show a 95% confidence interval. The models depict significant effects of NSR
491 and study year (2016-2018 with wet-to-dry climate, SPEI values in brackets) on the logarithm of basal
492 area increment (bai_{std}) of focal trees predicted for cavitation resistant (PC1 value of -1.5) and acquisitive
493 species (PC1 value of 1.5). The panels illustrate the influence of focal tree resistance-acquisition traits
494 (black tree; A, B) and neighbour resistance-acquisition traits (C) on the relationships. See Fig. 1 for
495 details on the study design and Tables S8,9 for details on the fitted models.

496

497 The stomatal control traits of focal trees significantly modulated relationships between climate
498 and growth but not between NSR and growth nor between NSR, climate and growth (Fig. 4A,
499 Table S11). Growth increased for water-saving species but decreased for water-spending
500 species from the wet-to-dry year (year × focal tree stomatal control traits, $t = -5.10$, $P < 0.001$;
501 Fig. 4A). The stomatal control traits of neighbours significantly influenced the relationship
502 between climate and growth: Focal trees in a neighbourhood dominated by water-saving species
503 grew better from the wet-to-dry year, while growth of focal trees in a water spending
504 neighbourhood declined (year × NWM of stomatal control, $t = -3.04$, $P = 0.002$; Fig. 4B, Table
505 S12). Growth responses for basal area increment described here were similar for tree-ring

506 width, except for a general decline in tree-ring width from 2016-2018 and with tree size,
507 presumably due to an age trend (Figs. S9-11). The 3-way interaction of NSR, year and the
508 resistance-acquisition traits of focal trees was significant for tree-ring width ($t = -2.21$, $P =$
509 0.027 ; Fig. S10).
510



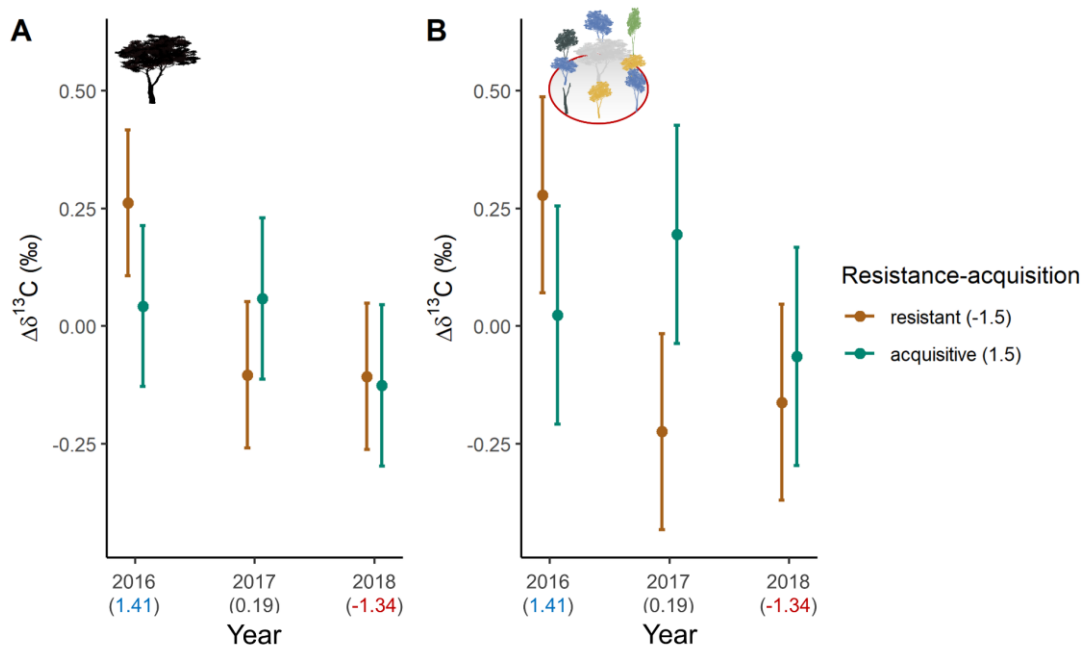
511
512 Fig. 4 Modulation of the relationship between climate and growth by stomatal control traits. Lines
513 represent linear mixed-effects model fits and coloured bands show a 95% confidence interval. The
514 models depict significant effects of study year (2016-2018 with wet-to-dry climate, SPEI values in
515 brackets) on the logarithm of basal area increment (bai_{std}) of focal trees predicted for water savers (PC2
516 value of -1.5) and water spenders (PC2 value of 1.0). The panels illustrate the influence of focal tree
517 stomatal control traits (black tree; A) and neighbour stomatal control traits (tree neighbourhood; B) on
518 the relationship. See Fig. 1 for details on the study design and Tables S11,12 for details on the fitted
519 models.

520

521 **The effect of drought-tolerance traits on $\delta^{13}\text{C}$**

522 Using trait-dependent models to explain variations in $\delta^{13}\text{C}$ in the wood of focal trees, we found
523 significant interactions of resistance-acquisition traits with climate, but the effect of neighbour

524 traits was stronger than that of focal tree traits (Fig. 5, Tables S13,14). In the intermediate- and
525 dry-year, we observed higher $\delta^{13}\text{C}$ (higher water stress) in focal trees in an acquisitive
526 neighbourhood than in a resistant one. However, lower $\delta^{13}\text{C}$ (lower water stress) occurred in
527 focal trees in an acquisitive neighbourhood in the wet year (year \times NWM of resistance-
528 acquisition, year as a categorical fixed effect, $F = 9.45$, $P < 0.001$; Fig. 5B). The difference
529 between focal trees in resistant *vs* acquisitive neighbourhoods was biggest in the year with
530 intermediate water availability (2017; Fig. 5B).
531

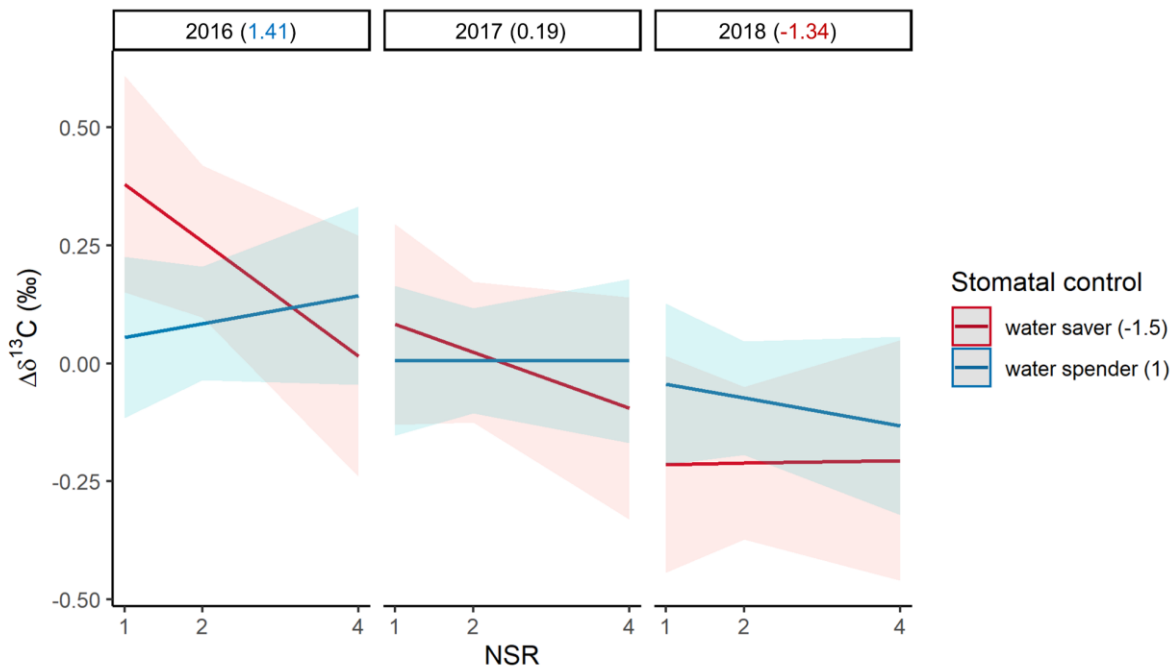


532
533 Fig. 5 Modulation of the relationship between climate and $\delta^{13}\text{C}$ by resistance-acquisition traits. Points
534 represent linear mixed-effects model fits and error bars show a 95% confidence interval. The models
535 depict significant effects of study year (2016-2018 with wet-to-dry climate, SPEI values in brackets) on
536 $\delta^{13}\text{C}$ in the wood of focal trees predicted for cavitation resistant (PC1 value of -1.5) and acquisitive
537 species (PC1 value of 1.5). The panels illustrate the influence of focal tree resistance-acquisition traits
538 (black tree; A) and neighbour resistance-acquisition traits (tree neighbourhood; B) on the relationship.
539 See Fig. 1 for details on the study design and Tables S13,14 for details on the fitted models.

540

541 The stomatal control traits of focal trees significantly modulated the relationship between NSR,
542 climate and $\delta^{13}\text{C}$ (NSR \times year \times focal tree stomatal control traits, $t = -2.66$, $P = 0.008$; Fig. 6,
543 Table S15): We found contrasting NSR effects on $\delta^{13}\text{C}$ for water-saving and water-spending
544 species, which weakened from wet-to-dry climatic conditions (Fig. 6). In the wet year, $\delta^{13}\text{C}$
545 decreased in water savers with increasing NSR. However, this positive diversity effect declined
546 towards similar $\delta^{13}\text{C}$ across NSR levels in the dry year. In contrast, water spending species
547 tended to show increasing $\delta^{13}\text{C}$ with increasing NSR in the wet year but decreasing $\delta^{13}\text{C}$ with
548 increasing NSR in the dry year. Hence, water savers benefited from more species-rich
549 neighbourhoods (NSR) via lower water stress during wet conditions. In contrast, water spenders
550 benefited from higher NSR during dry climatic conditions, even though effect sizes were
551 relatively small. Finally, stomatal control traits of neighbours influenced $\delta^{13}\text{C}$ in the wood of
552 focal trees (year \times NWM of stomatal control, $t = 3.43$, $P = 0.001$; Fig. S12, Table S16). Focal
553 trees in a water-saving neighbourhood had lower $\delta^{13}\text{C}$ in the dry than in the wet year, but this
554 effect was potentially enhanced by the overall decline in $\delta^{13}\text{C}$ from the wet-to-dry year (Fig.
555 S7).

556



557

558 Fig. 6 Modulation of the relationship between neighbourhood species richness (NSR), climate and $\delta^{13}\text{C}$
559 by stomatal control traits. Lines represent linear mixed-effects model fits and coloured bands show a
560 95% confidence interval. The models depict significant, interactive effects of NSR and study year (2016-
561 2018 with wet-to-dry climate, SPEI values in brackets) on $\delta^{13}\text{C}$ in the wood of focal trees predicted for
562 water savers (PC2 value of -1.5) and water spenders (PC2 value of 1.0). See Fig. 1 for details on the
563 study design and Table S15 for details on the fitted model.

564

565 Discussion

566 The growth of focal trees increased with neighbourhood tree species richness (NSR) across the
567 15 species examined. However, we did not find an overall significant effect of NSR on carbon
568 isotopic ratios in the wood of focal trees ($\delta^{13}\text{C}$), nor an increase in the strength of the relationship
569 between NSR and growth and between NSR and $\delta^{13}\text{C}$ from wet-to-dry climatic conditions.
570 Instead, relationships between NSR, climate and growth or $\delta^{13}\text{C}$ were modulated by drought-
571 tolerance traits of focal trees regarding cavitation resistance vs. resource acquisition and
572 stomatal control. Species with contrasting drought-tolerance traits showed opposite responses
573 to NSR and climate. Using trait-dependent tree neighbourhood models, we could further show

574 that the drought-tolerance traits of tree neighbours consistently changed the nature of focal tree
575 growth and $\delta^{13}\text{C}$ responses to climatic conditions. These changes by the traits of neighbours
576 operated in the same direction as the changes induced by the traits of focal trees, thereby
577 amplifying tree responses to climate. The biotic context, which we quantified in terms of
578 drought-tolerance traits of focal trees and their neighbours, thus determined the strength and
579 nature of BEF relationships in the examined tree communities.

580

581 **Tree diversity increases growth but does not universally relieve drought stress**

582 As postulated in H1, NSR increased growth, which is consistent with findings from other
583 studies (Guillemot et al., 2020; Schnabel et al., 2019; Trogisch et al., 2021), including those
584 from our experiment (Fichtner et al., 2018; Fichtner et al., 2020). Still, NSR effects on the
585 growth of individual species can be both positive and negative and vary with climatic conditions
586 (Fig. S6; e.g. Vitali et al., 2018). Tree growth is an integrated signal of many biotic and abiotic
587 drivers (Grossiord, 2020). The positive effect of NSR on growth is thus likely the result of
588 different and interacting mechanisms operating at the neighbourhood scale (Trogisch et al.,
589 2021). The positive interactions potentially include resource partitioning (of light, water and
590 nutrients), abiotic facilitation (such as microclimate amelioration) and biotic interactions (such
591 as dilution of generalist pathogens) (Barry et al., 2019).

592

593 Water stress in focal trees causes changes in the carbon isotope composition of wood, and we
594 thus consider $\delta^{13}\text{C}$ as a proxy for neighbourhood-scale water availability (Grossiord et al., 2014;
595 Jucker et al., 2017). Contrary to our expectation and an earlier study on twig $\delta^{13}\text{C}$ in our
596 experiment conducted during the particularly wet year 2015 (Fig. 1A; Jansen et al., 2021), we
597 did not detect an overall decrease in $\delta^{13}\text{C}$ with NSR and thus no general enhancement of water
598 availability in more diverse tree neighbourhoods. Similarly to our finding, other studies found
599 mixed results and no universal decrease in $\delta^{13}\text{C}$ in mixtures compared to monocultures

600 (Grossiord, 2020; Haberstroh & Werner, 2022). Jansen et al. (2021) found the strongest
601 relationship between NSR and $\delta^{13}\text{C}$ for trees with high a high degree of crown competition from
602 neighbours and only marginal effects for trees with low crown competition. We thus expect that
603 the net negative effect of NSR on $\delta^{13}\text{C}$ in their study resulted from increased shading at high
604 NSR and not from enhanced water availability. This interpretation is supported by the finding
605 that tree biomass and thus shading increased with species richness in BEF-China (Huang et al.,
606 2018). In contrast, our $\delta^{13}\text{C}$ values should be primarily influenced by climate-induced water
607 availability as we only studied (co-)dominant trees with slight shading, which is supported by
608 the non-significant effect of all competition indices (Table S7) on $\delta^{13}\text{C}$.

609

610 **Abiotic context dependency**

611 The abiotic context, such as inter-annual changes in water availability, may determine the
612 strength and nature of BEF relationships (e.g., Forrester & Bauhus, 2016). To analyse this
613 abiotic context dependency, we selected the years for our analysis based on standardised
614 climatic water balances which presented a gradient from wet-to-dry climatic conditions (SPEIs;
615 Fig. S1). This analysis of wet-to-dry years prevented negative carry-over effects of drought, but
616 positive carry-over effects from favourable years may have buffered drought impacts through
617 the mobilisation of carbon reserves (McDowell et al., 2022). Moreover, drought stress may
618 have been less severe than suggested by SPEIs. The dry year we examined had similar SPEIs
619 as past drought years (Fig. S2), but non-standardised climatic water balances were rarely
620 negative (Fig. S3). Together, these points may explain why we observed no overall decline in
621 tree growth and decreasing $\delta^{13}\text{C}$ values from the wet to the dry year. Hence, even though all
622 forest biomes, including the comparably humid subtropical forests examined here, are
623 threatened by drought (Hartmann et al., 2022), responses may be more pronounced during
624 extreme droughts (e.g. during hotter droughts; Schnabel et al., 2022).

625

626 We also expected that increasing NSR would benefit growth and relief water stress more with
627 increasingly limited water availability. Yet, we did not find such an overall increase in diversity
628 effects from wet-to-dry climatic conditions, suggesting that either water availability was not
629 limited, or that the diversity signal on water availability is only expressed in growth and $\delta^{13}\text{C}$
630 when water stress reaches a certain threshold. Alternatively, other resources than water, such
631 as light, may have been the more limiting factor in our study system (Forrester & Bauhus,
632 2016). Other experimental studies reported stronger diversity effects on growth during dry
633 (Fichtner et al., 2020; Schnabel et al., 2019) and during wet years (Belluau, Vitali, Parker,
634 Paquette, & Messier, 2021). Similarly, positive, neutral and negative effects of species richness
635 on growth and $\delta^{13}\text{C}$ have been reported under drought (Forrester et al., 2016; Grossiord et al.,
636 2014; Grossiord, 2020). One problem in this context is that it has been challenging to quantify
637 the type and intensity of stress causing changes in the strength and nature of BEF relationships.
638 Here, we attempted to address this by considering the biotic context dependency of BEF
639 relationships under drought.

640

641 **Biotic context dependency**

642 Trait-based neighbourhood models have been used to understand community assembly
643 (Kunstler et al., 2012; Uriarte et al., 2010) and in few cases to understand how focal tree traits
644 modulate responses to NSR and climate (e.g. Fichtner et al., 2020). However, despite
645 compelling arguments for why the traits of neighbouring trees may alter local water availability
646 (Forrester, 2017), we account here for the first time for both focal tree and neighbour traits and
647 thus the biotic context dependency of BEF relationships in experimental tree communities.

648

649 The omission of this biotic context, which reversed the direction of BEF relationships in our
650 study, could be one reason for the mixed results of former studies on tree diversity's role during
651 drought. Given the different drought-tolerance traits in the examined species, it is not surprising

652 that we detected a net zero or only a weak overall effect of NSR on focal tree responses in our
653 study as we examined a balanced sample (in terms of species and number of individuals;
654 N=336) along both drought-tolerance trait gradients (Fig. 1B). In contrast, a former study in
655 BEF-China found a strengthening of positive NSR effects on growth under dry conditions,
656 using census data of all inventoried trees (N=3397) without controlling for a balanced sample
657 of traits (Fichtner et al., 2020). Differences in drought severity between the examined dry years
658 (2011 in Fichtner et al. vs 2018 in our study) are unlikely to have caused these different results,
659 as climatic conditions were comparable (Fig. 1A). Instead, the contrasting water-use strategies
660 of focal trees and their neighbours may be one fundamental missing link for explaining
661 divergent results of tree responses to drought in mixed-species forests.

662

663 **The importance of focal tree traits**

664 Consistent with H2, we found that during drought, NSR increased growth and decreased wood
665 $\delta^{13}\text{C}$ of acquisitive (cavitation-sensitive) and water-spending focal tree species. Hence, high
666 neighbourhood diversity supported the more vulnerable species in the forest community during
667 drought (Fichtner et al., 2020). In contrast, cavitation-resistant and water-saving species did not
668 respond to NSR, presumably because their strategies to cope with drought were not aided by
669 species interactions. Moreover, acquisitive and water-spending species showed decreased
670 growth from the wet to the dry year, whereas in cavitation-resistant and water-saving species
671 growth increased.

672

673 In general, the likelihood of having heterospecific neighbours increases with increasing NSR.
674 This presence of heterospecific neighbours with different traits than the focal tree may have
675 influenced focal species responses by enhancing or reducing competition or promoting
676 facilitation (Forrester, 2017; Forrester & Pretzsch, 2015). In our study system, enhanced growth
677 of acquisitive focal species at high NSR is likely related to the higher ability of these species to

678 acquire and use resources such as light and water relative to their heterospecific (more
679 conservative) neighbours under wet and dry climatic conditions, respectively (Fichtner et al.,
680 2017; Fichtner et al., 2020). Our focus on (co-)dominant trees probably restricted our analysis
681 to conditions of low neighbourhood competition where acquisitive species benefit from high
682 NSR while conservative species do not (Fichtner et al., 2017). At high NSR, acquisitive
683 (cavitation-sensitive) species were thus protected by diversity, which mitigated drought stress
684 through lower inter- compared to intraspecific competition for water (Fichtner et al., 2020).
685 Moreover, growth responses to declining water availability were likely related not only to
686 resource acquisition but also to cavitation resistance, as cavitation-resistant species may have
687 been able to grow better under drought due to lower degrees of embolism in their vessels
688 (McDowell et al., 2008).

689
690 Similarly, water savers may have grown better during dry years as they faced lower cavitation
691 risks (McDowell et al., 2008), while water spenders may have grown better during wet years as
692 they were able to operate optimally without facing hydraulic damage. The lower physiological
693 water stress (lower $\delta^{13}\text{C}$) we found in water-spending species during drought at high NSR
694 indicates a novel drought mitigation effect of diversity in addition to the protection of
695 acquisitive species reported formerly (Fichtner et al., 2020). NSR may have relieved water
696 stress during drought as it increases the likelihood of having water-saving neighbours, which
697 transpire less water, thereby increasing local soil water availability (Forrester, 2017). In
698 contrast, during the wet year, where higher high soil moisture enables higher evapotranspiration
699 potentials (Frenne et al., 2021), water-saving species may have profited from NSR because they
700 benefitted from microclimate amelioration by water-spending neighbours (Forrester, 2017).
701 This finding also indicates that the tight stomatal regulation of water savers induces $\delta^{13}\text{C}$
702 responses already during short dry periods (negative climatic water balances appeared each
703 year; Fig. S3) (Jansen et al., 2021) and not only during prolonged drought periods.

704

705 **The importance of neighbour traits**

706 Consistent with H3, focal trees grew less in neighbourhoods dominated by acquisitive and
707 water-spending species during drought, while they grew more in resistant and water-saving
708 neighbourhoods. We also observed higher $\delta^{13}\text{C}$ values in focal trees in acquisitive
709 neighbourhoods during the intermediate- and dry-year. Both observations indicate reductions
710 in local water availability and thus enhanced water stress (Forrester, 2017; Grossiord et al.,
711 2014) in neighbourhoods dominated by acquisitive and water-spending species relative to
712 neighbourhoods dominated by resistant and water-saving species. This finding may be
713 explained by acquisitive and water-spending neighbours having a higher water consumption
714 during drought. Acquisitive species tend to have a high maximum xylem hydraulic conductance
715 (Bongers et al., 2021), while water spenders close their stomata only late during dry conditions
716 and thus continue to transpire and consume water (McDowell et al., 2008).

717

718 Fichtner et al. (2020) already suggested that reduced competition for water between
719 heterospecific neighbours benefits cavitation-sensitive species in diverse neighbourhoods. Still,
720 they could not test this assumption as they did not quantify the influence of neighbour traits.
721 Explicitly accounting for neighbour traits – instead of using neighbourhood species
722 composition as a random effect (e.g. Fichtner et al., 2020; Jansen et al., 2021) – allowed us to
723 quantify the influence of the functional identity of neighbourhoods and the influence of their
724 diversity.

725

726 **Coordination of drought-tolerance traits**

727 Resistance-acquisition traits primarily modulated climate and NSR effects on growth, whereas
728 stomatal control traits primarily influenced wood $\delta^{13}\text{C}$. As expected, growth was thus more
729 strongly related to the leaf economics spectrum (Reich, 2014), while $\delta^{13}\text{C}$ was controlled by

730 stomatal aperture (Farquhar et al., 1989). The orthogonality of the resistance-acquisition and
731 stomatal control gradient in our study system (Fig. 1B) allowed us to disentangle the respective
732 contributions of both gradients through exploring the effects of stomatal control (or resistance-
733 acquisition) traits at mean levels of the other gradient. The species responses in years with
734 different water availability were consistent with the current understanding of trade-offs between
735 high cavitation resistance (low Ψ_{50}) and acquisitive resource use (Guillemot et al., 2022; Reich,
736 2014) and between water-spending and water-saving stomatal control (Martínez-Vilalta
737 & Garcia-Forner, 2017). However, despite the orthogonality in our study system, some
738 association between resistance-acquisition and stomatal control traits may be expected in
739 general (e.g. Klein, 2014) but may not manifest itself in local studies (e.g. Laughlin et al., 2020),
740 as relationships between drought-tolerance traits likely depend on study extent and traits
741 measured. We discuss these points in detail in Supplementary Discussion 1.

742
743 Finally, other traits related to drought tolerance may have influenced the observed responses
744 despite our consideration of multiple traits. Such traits include the storage of non-structural
745 carbohydrates, which trees use for maintaining turgor and for defending themselves against
746 biotic agents (Hartmann et al., 2022; McDowell et al., 2022), and attributes of the root system
747 (Weigelt et al., 2021). For instance, carbohydrate storage influences diversity effects on tree
748 survival under drought (Hajek et al., 2022). Therefore, future studies should examine such traits
749 and their relationships with the herein-examined ones to provide a more holistic picture of tree
750 drought responses and their modulation by functional traits.

751

752 **Conclusion**

753 In a large-scale tree diversity experiment, we analysed tree growth and wood $\delta^{13}\text{C}$ responses to
754 contrasting climatic conditions for trees sampled along gradients in neighbourhood species

755 richness (NSR) and drought-tolerance traits. We found enhanced growth but no universal relief
756 of water stress in diverse tree neighbourhoods. Instead, drought tolerance traits related to
757 cavitation resistance vs. resource acquisition and stomatal control of focal trees and their
758 neighbours modulated the relationship between NSR and growth and between NSR and $\delta^{13}\text{C}$
759 under variable climatic conditions. We derived two key conclusions: (1) Considering the
760 functional identity of focal trees and their neighbours resolved the biotic context dependency
761 of BEF relationships; such a trait-based perspective may help to explain positive and negative
762 mixing effects under drought. (2) Drought-tolerance traits of focal trees and interactions with
763 their tree neighbours induced contrasting species responses to wet vs dry climatic conditions;
764 this trait-driven species asynchrony is a key driver of positive diversity-stability relationships
765 in forests (Schnabel et al., 2021). The biotic context we analysed using a trait-based approach,
766 with traits tailored to the target ecosystem functions assessed, may help to generalize the context
767 dependency of BEF relationships and is relevant for designing tree mixtures suitable to cope
768 with a range of different drought conditions. It can give insight into the optimal configuration
769 of tree neighbourhoods in terms of diversity and identity in drought-tolerance traits. This may
770 help to optimise forest productivity and foster stability to climate extremes.

771

772 **Acknowledgements**

773 We thank local workers, in particular Mr. Wang and Mr. Shi, for invaluable help in the field,
774 Luise Münsterberg, Paulina Tjandraputri and Lara Schmitt for supporting the sample
775 preparation for the carbon isotope analyses and Wenzel Kröber and Helge Bruelheide for trait
776 measurements. This research was supported by the International Research Training Group
777 TreeDi funded by the Deutsche Forschungsgemeinschaft (DFG, German Research Foundation)
778 – 319936945/GRK2324 and the University of Chinese Academy of Sciences.

779

780 **Conflict of interest**

781 The authors declare no conflicts of interest.

782

783 **Author contributions**

784 Florian Schnabel, Kathryn E. Barry, Anja Kahl, Joannès Guillemot, Jürgen Bauhus and
785 Christian Wirth conceived the ideas of the study and designed the methodology; Florian
786 Schnabel, Susanne Eckhardt, Heike Geilmann, Anja Kahl and Heiko Moossen collected the
787 data; Florian Schnabel and Susanne Eckhardt analysed the data and Kathryn E. Barry, Joannès
788 Guillemot, Jürgen Bauhus and Christian Wirth joined the interpretation of the data and results;
789 Florian Schnabel created the figures; Florian Schnabel wrote the manuscript; All authors
790 contributed critically to the drafts and gave final approval for publication.

791

792 **Data availability statement**

793 Tree growth and stable carbon isotope data are available from the BEF-China project database
794 (<https://data.botanik.uni-halle.de/bef-china>; data will be made publicly available before
795 publication). Climate and trait data are available from the Climatic Research Unit (CRU TS
796 v4.04; Harris et al., 2020) and from Kröber et al. (2014), respectively.

797

798 **References**

799 Anderegg, W. R. L., Trugman, A. T., Badgley, G., Anderson, C. M., Bartuska, A.,
800 Ciais, P., . . . Randerson, J. T. (2020). Climate-driven risks to the climate mitigation
801 potential of forests. *Science*, 368(6497). <https://doi.org/10.1126/science.aaz7005>
802 Barry, K. E., Mommer, L., van Ruijven, J., Wirth, C., Wright, A. J., Bai, Y., . . . Weigelt, A.
803 (2019). The Future of Complementarity: Disentangling Causes from Consequences. *Trends*
804 *in Ecology & Evolution*, 34(2), 167–180.

- 805 Bates, D., Mächler, M., Bolker, B., & Walker, S. (2015). Fitting Linear Mixed-Effects Models
806 Using lme4. *Journal of Statistical Software*, 67(1). <https://doi.org/10.18637/jss.v067.i01>
- 807 Belluau, M., Vitali, V., Parker, W., Paquette, A., & Messier, C. (2021). Overyielding in young
808 tree communities does not support the stress-gradient hypothesis and is favoured by
809 functional diversity and higher water availability. *Journal of Ecology*, 109(4).
810 <https://doi.org/10.1111/1365-2745.13602>
- 811 Bertness, M. D., & Callaway, R. (1994). Positive interactions in communities. *Trends in*
812 *Ecology & Evolution*, 9(5), 191–193. [https://doi.org/10.1016/0169-5347\(94\)90088-4](https://doi.org/10.1016/0169-5347(94)90088-4)
- 813 Biondi, F., & Qeadan, F. (2008). A Theory-Driven Approach to Tree-Ring Standardization:
814 Defining the Biological Trend from Expected Basal Area Increment. *Tree-Ring Research*,
815 64(2), 81–96. <https://doi.org/10.3959/2008-6.1>
- 816 Böhnke, M., Kreißig, N., Kröber, W., Fang, T., & Bruelheide, H. (2012). Wood trait-
817 environment relationships in a secondary forest succession in South-East China. *Trees*,
818 26(2), 641–651.
- 819 Bongers, F. J., Schmid, B., Bruelheide, H., Bongers, F., Li, S., Oheimb, G. von, . . . Liu, X.
820 (2021). Functional diversity effects on productivity increase with age in a forest biodiversity
821 experiment. *Nature Ecology & Evolution*. Advance online publication.
822 <https://doi.org/10.1038/s41559-021-01564-3>
- 823 Brancalion, P. H. S., Niamir, A., Broadbent, E., Crouzeilles, R., Barros, F. S. M., Almeyda
824 Zambrano, A. M., . . . Chazdon, R. L. (2019). Global restoration opportunities in tropical
825 rainforest landscapes. *Science Advances*, 5(7), eaav3223.
826 <https://doi.org/10.1126/sciadv.aav3223>
- 827 Bruelheide, H., Nadrowski, K., Assmann, T., Bauhus, J., Both, S., Buscot, F., . . . Schmid, B.
828 (2014). Designing forest biodiversity experiments: General considerations illustrated by a

- 829 new large experiment in subtropical China. *Methods in Ecology and Evolution*, 5(1), 74–89.
- 830 <https://doi.org/10.1111/2041-210X.12126>
- 831 Bunn, A. G., Korpela, M., Biondi, F., Campelo, F., Mérian, P., Qeadan, F., & Zang, C. (2020).
- 832 *dplR: Dendrochronology Program Library in R*. Retrieved from [https://CRAN.R-](https://CRAN.R-project.org/package=dplR)
- 833 [project.org/package=dplR](https://CRAN.R-project.org/package=dplR)
- 834 Choat, B., Jansen, S., Brodribb, T. J., Cochard, H., Delzon, S., Bhaskar, R., . . . Zanne, A. E.
- 835 (2012). Global convergence in the vulnerability of forests to drought. *Nature*, 491(7426),
- 836 752–755. <https://doi.org/10.1038/nature11688>
- 837 Coplen, T. B. (2011). Guidelines and recommended terms for expression of stable-isotope-ratio
- 838 and gas-ratio measurement results. *Rapid Communications in Mass Spectrometry: RCM*,
- 839 25(17), 2538–2560. <https://doi.org/10.1002/rcm.5129>
- 840 Coplen, T. B., Brand, W. A., Gehre, M., Gröning, M., Meijer, H. A. J., Toman, B., &
- 841 Verkouteren, R. M. (2006). New guidelines for delta13C measurements. *Analytical*
- 842 *Chemistry*, 78(7), 2439–2441. <https://doi.org/10.1021/ac052027c>
- 843 Craven, D., Eisenhauer, N., Pearse, W. D., Hautier, Y., Isbell, F., Roscher, C., . . . Manning, P.
- 844 (2018). Multiple facets of biodiversity drive the diversity–stability relationship. *Nature*
- 845 *Ecology & Evolution*, 2(10), 1579–1587. <https://doi.org/10.1038/s41559-018-0647-7>
- 846 Del Río, M., Pretzsch, H., Ruiz-Peinado, R., Jactel, H., Coll, L., Löf, M., . . . Bravo-Oviedo, A.
- 847 (2022). Emerging stability of forest productivity by mixing two species buffers temperature
- 848 destabilizing effect. *Journal of Applied Ecology*. Advance online publication.
- 849 <https://doi.org/10.1111/1365-2664.14267>
- 850 Farquhar, G. D., Ehleringer, J. R., & Hubick, K. T. (1989). Carbon Isotope Discrimination and
- 851 Photosynthesis. *Annual Review of Plant Physiology and Plant Molecular Biology*, 40(1),
- 852 503–537. <https://doi.org/10.1146/annurev.pp.40.060189.002443>

- 853 Fichtner, A., Härdtle, W., Bruelheide, H., Kunz, M., Li, Y. [Ying], & Oheimb, G. von (2018).
854 Neighbourhood interactions drive overyielding in mixed-species tree communities. *Nature*
855 *Communications*, 9(1), 1144. <https://doi.org/10.1038/s41467-018-03529-w>
- 856 Fichtner, A., Härdtle, W., Li, Y. [Ying], Bruelheide, H., Kunz, M., & Oheimb, G. von (2017).
857 From competition to facilitation: How tree species respond to neighbourhood diversity.
858 *Ecology Letters*, 20(7), 892–900. <https://doi.org/10.1111/ele.12786>
- 859 Fichtner, A., Schnabel, F., Bruelheide, H., Kunz, M., Mausolf, K., Schuldt, A., . . .
860 Oheimb, G. von (2020). Neighbourhood diversity mitigates drought impacts on tree growth.
861 *Journal of Ecology*, 108(3), 865–875. <https://doi.org/10.1111/1365-2745.13353>
- 862 Forrester, D. I. (2017). Ecological and Physiological Processes in Mixed Versus Monospecific
863 Stands. In H. Pretzsch, D. I. Forrester, & J. Bauhus (Eds.), *Mixed-species forests: Ecology*
864 *and management* (pp. 73–115). Berlin, Germany: Springer Nature.
- 865 Forrester, D. I., & Bauhus, J. (2016). A Review of Processes Behind Diversity—Productivity
866 Relationships in Forests. *Current Forestry Reports*, 2(1), 45–61.
867 <https://doi.org/10.1007/s40725-016-0031-2>
- 868 Forrester, D. I., Bonal, D., Dawud, S., Gessler, A., Granier, A., Pollastrini, M., & Grossiord, C.
869 (2016). Drought responses by individual tree species are not often correlated with tree
870 species diversity in European forests. *Journal of Applied Ecology*, 53(6), 1725–1734.
871 <https://doi.org/10.1111/1365-2664.12745>
- 872 Forrester, D. I., & Pretzsch, H. (2015). Tamm Review: On the strength of evidence when
873 comparing ecosystem functions of mixtures with monocultures. *Forest Ecology and*
874 *Management*, 356, 41–53. <https://doi.org/10.1016/j.foreco.2015.08.016>
- 875 Fortunel, C., Valencia, R., Wright, S. J., Garwood, N. C., & Kraft, N. J. B. (2016). Functional
876 trait differences influence neighbourhood interactions in a hyperdiverse Amazonian forest.
877 *Ecology Letters*, 19(9), 1062–1070. <https://doi.org/10.1111/ele.12642>

- 878 Frenne, P. de, Lenoir, J., Luoto, M., Scheffers, B. R., Zellweger, F., Aalto, J., . . . Hylander, K.
879 (2021). Forest microclimates and climate change: Importance, drivers and future research
880 agenda. *Global Change Biology*, 27(11), 2279–2297. <https://doi.org/10.1111/gcb.15569>
- 881 Gärtner, H., & Nievergelt, D. (2010). The core-microtome: A new tool for surface preparation
882 on cores and time series analysis of varying cell parameters. *Dendrochronologia*, 28(2), 85–
883 92. <https://doi.org/10.1016/j.dendro.2009.09.002>
- 884 Gheyret, G., Zhang, H.-T., Guo, Y., Liu, T.-Y., Bai, Y.-H., Li, S., . . . Tang, Z. (2021). Radial
885 growth response of trees to seasonal soil humidity in a subtropical forest. *Basic and Applied*
886 *Ecology*, 55, 74–86. <https://doi.org/10.1016/j.baae.2021.02.015>
- 887 Grams, T. E. E., Kozovits, A. R., Häberle, K.-H., Matyssek, R., & Dawson, T. E. (2007).
888 Combining delta 13 C and delta 18 O analyses to unravel competition, CO₂ and O₃ effects
889 on the physiological performance of different-aged trees. *Plant, Cell and Environment*,
890 30(8), 1023–1034. <https://doi.org/10.1111/j.1365-3040.2007.01696.x>
- 891 Grossiord, C. (2020). Having the right neighbors: How tree species diversity modulates drought
892 impacts on forests. *New Phytologist*, 228(1), 42–49. <https://doi.org/10.1111/nph.15667>
- 893 Grossiord, C., Granier, A., Ratcliffe, S., Bouriaud, O., Bruelheide, H., Checko, E., . . .
894 Gessler, A. (2014). Tree diversity does not always improve resistance of forest ecosystems
895 to drought. *Proceedings of the National Academy of Sciences of the United States of*
896 *America*, 111(41), 14812–14815. <https://doi.org/10.1073/pnas.1411970111>
- 897 Guillemot, J., Kunz, M., Schnabel, F., Fichtner, A., Madsen, C. P., Gebauer, T., . . . Potvin, C.
898 (2020). Neighbourhood-mediated shifts in tree biomass allocation drive overyielding in
899 tropical species mixtures. *New Phytologist*, 228(4), 1256–1268.
900 <https://doi.org/10.1111/nph.16722>
- 901 Guillemot, J., Martin-StPaul, N., Bulascoschi, L., Poorter, L., Morin, X., Pinho, B. X., . . .
902 Brancalion, P. H. S. (2022). Small and slow is safe: On the drought tolerance of tropical tree

903 species. *Global Change Biology*. Advance online publication.
904 <https://doi.org/10.1111/gcb.16082>

905 Haberstroh, S., & Werner, C. (2022). The role of species interactions for forest resilience to
906 drought. *Plant Biology*. Advance online publication. <https://doi.org/10.1111/plb.13415>

907 Hajek, P., Link, R. M., Nock, C. A., Bauhus, J., Gebauer, T., Gessler, A., . . . Schuldt, B.
908 (2022). Mutually inclusive mechanisms of drought-induced tree mortality. *Global Change*
909 *Biology*, 28(10), 3365–3378. <https://doi.org/10.1111/gcb.16146>

910 Hammond, W. M., Williams, A. P., Abatzoglou, J. T., Adams, H. D., Klein, T., López, R., . . .
911 Allen, C. D. (2022). Global field observations of tree die-off reveal hotter-drought
912 fingerprint for Earth's forests. *Nature Communications*, 13(1), 1761.
913 <https://doi.org/10.1038/s41467-022-29289-2>

914 Harris, I., Osborn, T. J., Jones, P., & Lister, D. (2020). Version 4 of the CRU TS monthly high-
915 resolution gridded multivariate climate dataset. *Scientific Data*, 7(1), 109.
916 <https://doi.org/10.1038/s41597-020-0453-3>

917 Hartmann, H., Bastos, A., Das, A. J., Esquivel-Muelbert, A., Hammond, W. M., Martínez-
918 Vilalta, J., . . . Allen, C. D. (2022). Climate Change Risks to Global Forest Health:
919 Emergence of Unexpected Events of Elevated Tree Mortality Worldwide. *Annual Review of*
920 *Plant Biology*. Advance online publication. [https://doi.org/10.1146/annurev-arplant-](https://doi.org/10.1146/annurev-arplant-102820-012804)
921 [102820-012804](https://doi.org/10.1146/annurev-arplant-102820-012804)

922 Huang, Y., Chen, Y., Castro-Izaguirre, N., Baruffol, M., Brezzi, M., Lang, A., . . . Schmid, B.
923 (2018). Impacts of species richness on productivity in a large-scale subtropical forest
924 experiment. *Science*, 362(6410), 80–83. <https://doi.org/10.1126/science.aat6405>

925 IPCC (2014). *Climate change 2014. Impacts, Adaptation, and Vulnerability. Part A: Global*
926 *and Sectoral Aspects. Contribution of Working Group II to the Fifth Assessment Report of*

- 927 *the Intergovernmental Panel on Climate Change*. New York, NY: Cambridge University
928 Press.
- 929 Jansen, K., Oheimb, G. von, Bruelheide, H., Härdtle, W., & Fichtner, A. (2021). Tree species
930 richness modulates water supply in the local tree neighbourhood: Evidence from wood $\delta^{13}\text{C}$
931 signatures in a large-scale forest experiment. *Proceedings. Biological Sciences*, 288(1946),
932 20203100. <https://doi.org/10.1098/rspb.2020.3100>
- 933 Jucker, T., Avacaritei, D., Barnoaiea, I., Duduman, G., Bouriaud, O., & Coomes, D. A. (2016).
934 Climate modulates the effects of tree diversity on forest productivity. *Journal of Ecology*,
935 104(2), 388–398. <https://doi.org/10.1111/1365-2745.12522>
- 936 Jucker, T., Grossiord, C., Bonal, D., Bouriaud, O., Gessler, A., & Coomes, D. A. (2017).
937 Detecting the fingerprint of drought across Europe’s forests: do carbon isotope ratios and
938 stem growth rates tell similar stories? *Forest Ecosystems*, 4(1), 706.
939 <https://doi.org/10.1186/s40663-017-0111-1>
- 940 Klein, T. (2014). The variability of stomatal sensitivity to leaf water potential across tree
941 species indicates a continuum between isohydric and anisohydric behaviours. *Functional*
942 *Ecology*, 28(6), 1313–1320. <https://doi.org/10.1111/1365-2435.12289>
- 943 Kröber, W., & Bruelheide, H. (2014). Transpiration and stomatal control: a cross-species study
944 of leaf traits in 39 evergreen and deciduous broadleaved subtropical tree species. *Trees*,
945 28(3), 901–914. <https://doi.org/10.1007/s00468-014-1004-3>
- 946 Kröber, W., Zhang, S., Ehmiq, M., & Bruelheide, H. (2014). Linking xylem hydraulic
947 conductivity and vulnerability to the leaf economics spectrum--a cross-species study of 39
948 evergreen and deciduous broadleaved subtropical tree species. *PLoS ONE*, 9(11), e109211.
949 <https://doi.org/10.1371/journal.pone.0109211>
- 950 Kunstler, G., Lavergne, S., Courbaud, B., Thuiller, W., Vieilledent, G.,
951 Zimmermann, N. E., . . . Coomes, D. A. (2012). Competitive interactions between forest

952 trees are driven by species' trait hierarchy, not phylogenetic or functional similarity:
953 Implications for forest community assembly. *Ecology Letters*, 15(8), 831–840.
954 <https://doi.org/10.1111/j.1461-0248.2012.01803.x>

955 Kuznetsova, A., Brockhoff, P. B., & Christensen, R. H. B. (2017). lmerTest Package: Tests in
956 Linear Mixed Effects Models. *Journal of Statistical Software*, 82(13).
957 <https://doi.org/10.18637/jss.v082.i13>

958 Laughlin, D. C., Delzon, S., Clearwater, M. J., Bellingham, P. J., McGlone, M. S., &
959 Richardson, S. J. (2020). Climatic limits of temperate rainforest tree species are explained
960 by xylem embolism resistance among angiosperms but not among conifers. *New Phytologist*,
961 226(3), 727–740. <https://doi.org/10.1111/nph.16448>

962 Li, Y. [Ying], Kröber, W., Bruelheide, H., Härdtle, W., & Oheimb, G. von (2017). Crown and
963 leaf traits as predictors of subtropical tree sapling growth rates. *Journal of Plant Ecology*,
964 10(1), 136–145. <https://doi.org/10.1093/jpe/rtw041>

965 Loader, N. J., Robertson, I., & McCarroll, D. (2003). Comparison of stable carbon isotope
966 ratios in the whole wood, cellulose and lignin of oak tree-rings. *Palaeogeography,*
967 *Palaeoclimatology, Palaeoecology*, 196(3-4), 395–407. [https://doi.org/10.1016/S0031-](https://doi.org/10.1016/S0031-0182(03)00466-8)
968 [0182\(03\)00466-8](https://doi.org/10.1016/S0031-0182(03)00466-8)

969 Martínez-Vilalta, J., & Garcia-Fornier, N. (2017). Water potential regulation, stomatal
970 behaviour and hydraulic transport under drought: Deconstructing the iso/anisohydric
971 concept. *Plant, Cell and Environment*, 40(6), 962–976. <https://doi.org/10.1111/pce.12846>

972 McDowell, N. G., Pockman, W. T., Allen, C. D., Breshears, D. D., Cobb, N., Kolb, T., . . .
973 Yezpez, E. A. (2008). Mechanisms of plant survival and mortality during drought: Why do
974 some plants survive while others succumb to drought? *New Phytologist*, 178(4), 719–739.
975 <https://doi.org/10.1111/j.1469-8137.2008.02436.x>

- 976 McDowell, N. G., Sapes, G., Pivovarov, A., Adams, H. D., Allen, C. D.,
977 Anderegg, W. R. L., . . . Xu, C. (2022). Mechanisms of woody-plant mortality under rising
978 drought, CO₂ and vapour pressure deficit. *Nature Reviews Earth and Environment*, 3, 294–
979 308. <https://doi.org/10.1038/s43017-022-00272-1>
- 980 Messier, C., Bauhus, J., Sousa-Silva, R., Auge, H., Baeten, L., Barsoum, N., . . . Zemp, D. C.
981 (2021). For the sake of resilience and multifunctionality, let's diversify planted forests!
982 *Conservation Letters*, 15(1), e12829. <https://doi.org/10.1111/conl.12829>
- 983 Paquette, A., & Messier, C. (2011). The effect of biodiversity on tree productivity: From
984 temperate to boreal forests. *Global Ecology and Biogeography*, 20(1), 170–180.
985 <https://doi.org/10.1111/j.1466-8238.2010.00592.x>
- 986 Reich, P. B. (2014). The world-wide ‘fast-slow’ plant economics spectrum: a traits manifesto.
987 *Journal of Ecology*, 102(2), 275–301. <https://doi.org/10.1111/1365-2745.12211>
- 988 Schnabel, F., Liu, X., Kunz, M., Barry, K. E., Bongers, F. J., Bruelheide, H., . . . Wirth, C.
989 (2021). Species richness stabilizes productivity via asynchrony and drought-tolerance
990 diversity in a large-scale tree biodiversity experiment. *Science Advances*, 7(51).
991 <https://doi.org/10.1126/sciadv.abk1643>
- 992 Schnabel, F., Purruicker, S., Schmitt, L., Engelmann, R. A., Kahl, A., Richter, R., . . . Wirth, C.
993 (2022). Cumulative growth and stress responses to the 2018-2019 drought in a European
994 floodplain forest. *Global Change Biology*, 28(5), 1870–1883.
995 <https://doi.org/10.1111/gcb.16028>
- 996 Schnabel, F., Schwarz, J. A., Dănescu, A., Fichtner, A., Nock, C. A., Bauhus, J., & Potvin, C.
997 (2019). Drivers of productivity and its temporal stability in a tropical tree diversity
998 experiment. *Global Change Biology*, 25(12), 4257-4272. <https://doi.org/10.1111/gcb.14792>
- 999 Schulze, B., Wirth, C., Linke, P., Brand, W. A., Kuhlmann, I., Horna, V., & Schulze, E.-D.
1000 (2004). Laser ablation-combustion-GC-IRMS--a new method for online analysis of intra-

- 1001 annual variation of delta13C in tree rings. *Tree Physiology*, 24(11), 1193–1201.
1002 <https://doi.org/10.1093/treephys/24.11.1193>
- 1003 Schwarz, J. A., Skiadaresis, G., Kohler, M., Kunz, J., Schnabel, F., Vitali, V., & Bauhus, J.
1004 (2020). Quantifying Growth Responses of Trees to Drought—a Critique of Commonly Used
1005 Resilience Indices and Recommendations for Future Studies. *Current Forestry Reports*, 6,
1006 185–200. <https://doi.org/10.1007/s40725-020-00119-2>
- 1007 Schweingruber, F. H. (1996). *Tree rings and environment: dendroecology*. Berne, Switzerland:
1008 Paul Haupt AG Bern.
- 1009 Shi, M.-M., Michalski, S. G., Welk, E., Chen, X.-Y., & Durka, W. (2014). Phylogeography of
1010 a widespread Asian subtropical tree: genetic east-west differentiation and climate envelope
1011 modelling suggest multiple glacial refugia. *Journal of Biogeography*, 41(9), 1710–1720.
1012 <https://doi.org/10.1111/jbi.12322>
- 1013 Stoll, P., & Newbery, D. M. (2005). Evidence of species-specific neighborhood effects in the
1014 dipterocarpaceae of a Bornean rain forest. *Ecology*, 86(11), 3048–3062.
1015 <https://doi.org/10.1890/04-1540>
- 1016 Trogisch, S., Liu, X., Rutten, G., Xue, K., Bauhus, J., Brose, U., . . . Bruelheide, H. (2021). The
1017 significance of tree-tree interactions for forest ecosystem functioning. *Basic and Applied*
1018 *Ecology*, 55, 33–52. <https://doi.org/10.1016/j.baae.2021.02.003>
- 1019 Uriarte, M., Swenson, N. G., Chazdon, R. L., Comita, L. S., John Kress, W., Erickson, D., . . .
1020 Thompson, J. (2010). Trait similarity, shared ancestry and the structure of neighbourhood
1021 interactions in a subtropical wet forest: Implications for community assembly. *Ecology*
1022 *Letters*, 13(12), 1503–1514. <https://doi.org/10.1111/j.1461-0248.2010.01541.x>
- 1023 Van der Plas, F. (2019). Biodiversity and ecosystem functioning in naturally assembled
1024 communities. *Biological Reviews*, 94(4), 1220–1245. <https://doi.org/10.1111/brv.12499>

- 1025 Vicente-Serrano, S. M., Beguería, S., & López-Moreno, J. I. (2010). A Multiscalar Drought
1026 Index Sensitive to Global Warming: The Standardized Precipitation Evapotranspiration
1027 Index. *Journal of Climate*, 23(7), 1696–1718. <https://doi.org/10.1175/2009JCLI2909.1>
- 1028 Vitali, V., Forrester, D. I., & Bauhus, J. (2018). Know Your Neighbours: Drought Response of
1029 Norway Spruce, Silver Fir and Douglas Fir in Mixed Forests Depends on Species Identity
1030 and Diversity of Tree Neighbourhoods. *Ecosystems*, 21(6), 1215–1229.
1031 <https://doi.org/10.1007/s10021-017-0214-0>
- 1032 Wang, X.-H., Kent, M., & Fang, X.-F. (2007). Evergreen broad-leaved forest in Eastern China:
1033 Its ecology and conservation and the importance of resprouting in forest restoration. *Forest
1034 Ecology and Management*, 245(1-3), 76–87. <https://doi.org/10.1016/j.foreco.2007.03.043>
- 1035 Weigelt, A., Mommer, L., Andraczek, K., Iversen, C. M., Bergmann, J., Bruelheide, H., . . .
1036 McCormack, M. L. (2021). An integrated framework of plant form and function: The
1037 belowground perspective. *New Phytologist*, 232(1), 42–59.
1038 <https://doi.org/10.1111/nph.17590>
- 1039 Werner, R. A., & Brand, W. A. (2001). Referencing strategies and techniques in stable isotope
1040 ratio analysis. *Rapid Communications in Mass Spectrometry: RCM*, 15(7), 501–519.
1041 <https://doi.org/10.1002/rcm.258>
- 1042 Yang, X., Bauhus, J., Both, S., Fang, T., Härdtle, W., Kröber, W., . . . Bruelheide, H. (2013).
1043 Establishment success in a forest biodiversity and ecosystem functioning experiment in
1044 subtropical China (BEF-China). *European Journal of Forest Research*, 132(4), 593–606.
1045 <https://doi.org/10.1007/s10342-013-0696-z>